

Galaxy Cluster Baryon Fractions, Cluster Surveys and Cosmology

Plenary contribution to PASCOS99 meeting, December, 1999

Joseph J. Mohr^{‡a}, Zoltan Haiman^{†b} & Gilbert P. Holder[‡]
[‡]*University of Chicago Department of Astronomy and Astrophysics*
[†]*Princeton University Observatory*

The properties of nearby galaxy clusters limit the range of cosmological parameters consistent with our universe. We describe the limits which arise from studies of the intracluster medium (ICM) mass fraction f_{ICM} and consideration of the possible sources of systematic error: $\Omega_M < 0.44h_{50}^{-1/2}$ at 95% confidence. We emphasize that independent of Type Ia supernovae (SNe Ia) observations, this cluster study, taken together with published cosmic microwave background (CMB) anisotropy studies, indicates a non-zero quintessence or dark energy component $\Omega_Q > 0$. We then discuss future galaxy cluster surveys which will probe the abundance of galaxy clusters to intermediate and high redshift. We investigate the sensitivity of these surveys to the cosmological density parameter Ω_M and the equation of state parameter w of any quintessence component. In particular, we show that cluster survey constraints from a proposed large solid angle X-ray survey are comparable in precision and complementary in nature to constraints expected from future CMB anisotropy and SNe Ia studies.

1 Overview

Galaxy clusters contain a wealth of accessible cosmological information. Their masses range from 10^{14} - $10^{15} M_\odot$, making clusters the most massive collapsed or virialized objects in the universe. Although numerous careful and varied studies of nearby clusters indicate that they are still accreting mass at the present epoch^{17,19,12,27}, it is evident that clusters exhibit striking regularity in scaling relations between mass, size and temperature^{28,29,23}. In fact the scatter of clusters about the X-ray size-temperature relation is 15%, comparable to the scatter of elliptical galaxies around the fundamental plane²⁴.

Both these characteristics (accretion at the present epoch and tight scaling relations) are also exhibited by clusters formed within hydrodynamical simulations^{14,15,5}, providing some confidence that the process of cluster formation is dominated by gravity and gas dynamics, and therefore simple enough to be effectively modeled in numerical simulations¹⁸. Ongoing observations with new X-ray observatories and proposed radio observatories will enable us to further improve our understanding of cluster formation and evolution^{36,35}. Because galaxy clusters are sufficiently regular that their masses can be esti-

^aChandra Fellow

^bHubble Fellow

mated from observables such as the ICM temperature T_x , yields from cluster surveys of the high redshift universe are more readily interpreted and can, in principle, be used to constrain cosmological parameters.

2 Constraints on Ω_M from ICM Mass Fractions

Galaxy clusters can be used to study the mix of baryonic and dark matter on scales of roughly 10 Mpc. Because there are no candidate mechanisms available to segregate baryons and dark matter on these scales¹⁶, it is often argued that the baryon fraction within clusters f_{cl} should reflect the universal baryon fraction $f_B \equiv \Omega_B/\Omega_M$, where Ω_B (Ω_M) is the cosmological density parameter of baryons (all clustered matter). Therefore, a measure of the cluster baryon fraction f_{cl} can be combined with primordial nucleosynthesis constraints on the baryon to photon ratio and measurements of the CMB temperature to yield an estimate of the cosmological density parameter $\Omega_M = \Omega_B/f_{cl}$ ⁴⁰.

There are at least three reservoirs of baryons in galaxy clusters: (1) the ICM, (2) the galaxies, and (3) dark baryons. The X-ray bremsstrahlung and recombination radiation from the ICM provides a precision tool for estimating the baryonic mass in the ICM reservoir. The optical light emitted by stars within galaxies provides a more blunt estimate of the baryonic mass in galaxies (requires accurate estimates of the baryonic mass to light ratio in typical cluster galaxies), and to date there is no clean way of separating a possible dark baryonic component from the dominant dark matter reservoir within clusters. Detailed studies of individual clusters tend to indicate that the ICM mass is several times larger than the galaxy mass¹⁰. Below we describe a study which uses observations of the ICM baryon reservoir to place an upper limit on Ω_M .

2.1 Study of the ICM in an X-ray Flux Limited Sample of 45 Clusters

The ICM density profile $\rho(r)$ can be extracted from an image of the cluster X-ray emission, given an estimate of the mean ICM temperature T_x , an emission model and some assumption about the cluster geometry. The central X-ray surface brightness can be expressed

$$I_x = \frac{1}{2\pi(1+z)^4} \int_0^\infty dl \frac{\rho(r)}{\mu_e \mu_H m_p^2} \Lambda(T_x), \quad (1)$$

where Λ is an emission coefficient, z is redshift, m_p is the proton rest mass, $n_i \equiv \rho/\mu_i$, and n_i is the number density of species i . We use ROSAT PSPC observations of 45 clusters from an X-ray flux limited sample with available data¹³. Within our chosen PSPC band (0.5:2 keV), the emission coefficient

Λ is extremely insensitive to ICM temperature²⁹, and so one can accurately infer $\rho(r)$ without direct knowledge of the ICM temperature structure. One does need to assume a geometry; we assume the clusters are spherical. This introduces errors in the density inversion, and we characterize these errors by testing our analysis on mock observations of simulated galaxy clusters. Using mock observations of 48 hydrodynamical simulations, we calculate that the cluster ICM mass within a radius r_{500} , roughly half the virial radius, can be estimated with an accuracy of 10%²⁹.

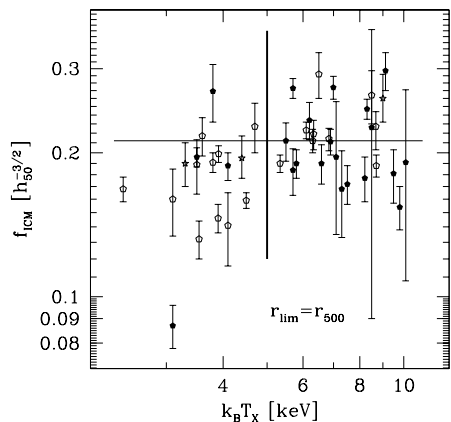


Figure 1: Measured ICM mass fractions f_{ICM} versus mean ICM temperature T_x for an X-ray flux limited sample of clusters. The mean f_{ICM} for the clusters with $k_B T_x > 5$ keV (vertical line) is $0.212 h_{50}^{-3/2}$ (horizontal line). This measurement provides a lower limit on the fraction of matter within cluster virial regions which is baryonic. Together with current best estimates of the scale of systematic errors on this upper limit, this measure of $\langle f_{ICM} \rangle$ provides a 95% confidence upper limit on the cosmological density parameter of clustered matter: $\Omega_M < 0.44 h_{50}^{-1/2}$.

To estimate the ICM mass fraction f_{ICM} we not only need the ICM density profile $\rho(r)$, but we also need the cluster binding mass. We estimate M_{500} , the binding mass within r_{500} , by assuming the ICM is in hydrostatic equilibrium and is isothermal. Departures from equilibrium and isothermality will introduce errors. A common temperature profile in clusters could potentially lead to systematic errors in our binding mass estimates. These are considered below in § 2.2.

Fig. 1 contains a plot of our f_{ICM} measurements versus emission weighted mean ICM temperature T_x in 45 clusters. There are two important characteristics of the distribution of f_{ICM} . First, there is a weak, but statistically significant, tendency for low mass (low $k_B T_x$) clusters to have lower f_{ICM} . The physics responsible for depleting the ICM in low mass clusters is thought to be preheating of the intergalactic medium by star formation within galaxies before the gas collapsed into the forming potential wells of clusters^{9,34}. Generally speaking, preheating of the gas prior to cluster formation or energy injection after cluster formation will have a larger effect on low mass clusters than on high. Thus, in using f_{ICM} to constrain the density of clustered matter, we restrict ourselves to the highest mass, hottest systems: $k_B T_x > 5$ keV.

Second, splitting the sample at 5 keV (vertical line), we find the mean

$f_{ICM} = (0.212 \pm 0.006)h_{50}^{-3/2}$ (the horizontal line). This number is in reasonably good agreement with other estimates of f_{ICM} ^{41,10,3}. Constraints on the primordial deuterium abundance from high redshift absorption systems provide an estimate of the baryon density parameter: $\Omega_B = 0.076h_{50}^2$ ⁷. Together with our lower limit on the cluster baryon fraction f_{cl} , this number implies an upper limit $\Omega_M < (0.36 \pm 0.01)h_{50}^{-1/2}$, where the uncertainty is only statistical. We require a factor of three systematic error to reconcile this number with $\Omega_M = 1$ cosmological models.

2.2 Discussion of Systematics

It is particularly interesting to consider systematics which could potentially make $\Omega_M = 1$ models more consistent with our data. There are several possible systematics: (1) any mechanism which enhances the cluster baryon fraction relative to the universal baryon fraction, (2) overestimating the ICM mass, and (3) underestimating the cluster binding mass M_{500} .

First, there are no known mechanisms for enhancing the baryon fraction by a factor of three on scales of 10 Mpc¹⁶. Second, plausible effects which would cause us to overestimate the ICM mass are (a) the effective area of the ROSAT PSPC is known to only 15%, corresponding to a 7.5% systematic uncertainty in our measured ICM masses, and (b) clumping or multiphase structure in the ICM would enhance the X-ray emission relative to single phase gas. In fact, our hydro simulations indicate that the X-ray emission is enhanced by roughly 20% on average by clumping in the gas³⁰; this leads us to overestimate the ICM mass by 10%, on average (we have already corrected for this). Interestingly, preliminary results from an ongoing analysis of an independent set of hydro simulations indicates that clumping from infalling substructure is present at about the same level as seen in our simulations⁶. In addition, this clumping can potentially be addressed by comparison of ICM mass fractions derived from X-ray data and those derived from Sunyaev-Zel'dovich Effect (SZE) observations. Because the SZE is sensitive to a line integral of the ρT_e , where T_e is the electron temperature, clumping would likely have a much stronger effect on the X-ray measures than on the SZE. A comparison of f_{ICM} derived from an analysis of SZE observations of 18 clusters provides no indication for systematically different results within an accepted range of the Hubble parameter H_0 ²⁰.

Third, there are many possible effects which could systematically affect our binding mass estimates M_{500} ; these include bulk flow or turbulence, support from magnetic fields, and ICM temperature profiles. Indeed, analyses of some individual clusters provides binding masses derived from galaxy dynamics

which are significantly higher than those derived from hydrostatic equilibrium. However, a systematic study by the CNOC collaboration of 14 intermediate redshift clusters finds the ratio of galaxy dynamical to isothermal hydrostatic masses to be 1.04 ± 0.07 ²⁵. Further studies using gravitational lensing and the spatially resolved ICM temperatures available from Chandra should provide much needed additional information.

Taking the 7.5% systematic from the uncertainty in the PSPC effective area and the 7% systematic uncertainty on the binding mass estimates, we estimate a total systematic uncertainty of 10%. This together with the observations outlined in the previous section leads to a 95% confidence upper limit of $\Omega_M < 0.44h_{50}^{-1/2}$.

2.3 Two Independent Observational Arguments for $\Omega_Q > 0$

Studies of high redshift SNe Ia prefer cosmological models with $\Omega_Q > 0$ ^{38,33}. Both cluster baryon fraction arguments and mass to light studies⁸ favor low Ω_M models. The mass to light ratio studies are more difficult to interpret, because the stellar populations of galaxies inside clusters differ significantly from those outside clusters. Nevertheless, these two approaches, subject to different systematics, indicate $\Omega_M \ll 1$. Together with constraints on CMB anisotropy¹¹, these clusters lead to the conclusion $\Omega_Q > 0$, independent of the SNe Ia studies.

3 Cluster Surveys and Cosmology

The relatively simple evolution (compared to galaxies) and regularity of galaxy clusters make them candidate tracer particles to use in measuring the volume–redshift relation. This classical cosmological test³⁹ has been applied to galaxies with limited success, due at least in part to the complex relation between galaxy brightness and mass and the poorly understood evolution of the galaxy abundance²⁶ (but see Newman & Davis article for discussion of new approach being considered in the DEEP survey). Clusters are more amenable to these studies, because our theoretical understanding of their structure and evolution is more complete. We don't expect the abundance of clusters to remain constant with redshift, but we can calculate its evolution, enabling the volume–redshift relation test. Moreover, the cosmological sensitivity of the abundance evolution itself provides additional leverage.

Galaxy cluster surveys of the nearby universe are an old endeavor¹; however, new technology and techniques are now making it possible to carry out extensive cluster studies of the intermediate and high redshift universe. Studies of particular interest include: (1) a 400 deg² serendipitous XMM cluster

survey extending to high redshift³⁷, (2) the 10^4 deg^2 survey of the nearby and intermediate redshift universe with the Sloan Digital Sky Survey (SDSS)², (3) a 12 deg^2 interferometric SZE survey of the high redshift universe^{29,22}, and (4) a 10^4 deg^2 , deep X-ray survey of the nearby and intermediate redshift universe.

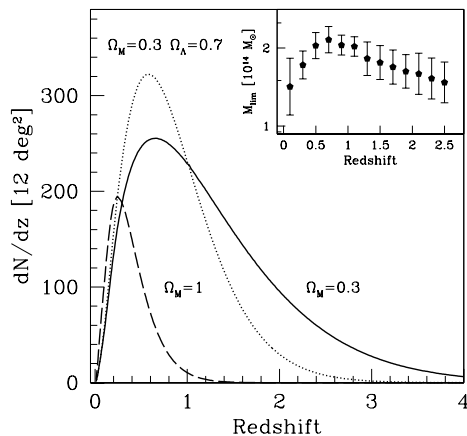


Figure 2: We plot the expected redshift distribution of a proposed SZE survey for three different cosmological models. The inset (upper right) shows the mass of clusters detectable at 5σ significance as a function of redshift. Note the mild redshift sensitivity of this mass threshold; this is the unique characteristic of an SZE survey. This particular proposed interferometric SZE survey will cover 12 deg^2 in one year, and it should yield a sample of roughly 400 clusters if the currently favored cosmological model ($\Omega_M = 0.3$, $\Omega_\Lambda = 0.7$, $\sigma_8 = 1$) is correct.

Fig 2 contains expectations for the redshift distribution of the interferometric SZE survey proposed by J. Carlstrom and collaborators. Because the SZE is a distortion of the CMB spectrum caused by inverse Compton scattering of CMB photons with hot electrons in the ICM, the SZE doesn't suffer from the cosmological dimming that any light source experiences. This fact makes the SZE ideally suited to studies of massive structures in the high redshift universe. The inset of Fig 2 contains the mass of a cluster which would be detected with 5σ significance as a function of redshift²². Interestingly, this limiting mass is relatively constant with redshift, and it corresponds to a very low mass galaxy cluster; thus, the proposed Carlstrom survey will enable us to probe the universe for clusters to the very moment of their emergence. As described below, this fundamental observation will provide a powerful test of structure formation models and allow precision measurements of several cosmological parameters.

3.1 Constraining the Equation of State Parameter w

Because there are now two independent observational arguments for a non-zero quintessence or dark energy component Ω_Q , further work is required not only to test this conclusion, but also to make measurements of the equation of state parameter $w \equiv p/\rho$ of this component. In principle the proposed SZE survey

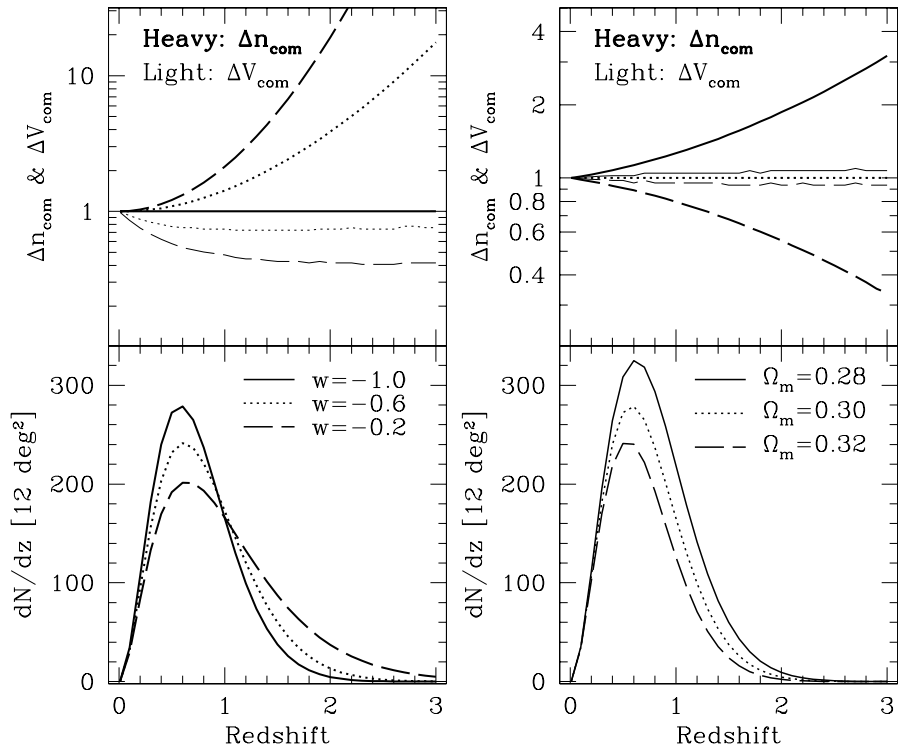


Figure 3: We show the sensitivity of an SZE survey to changing w (left) and changing Ω_M (right). These differences are separated (top) into the effects on the volume surveyed and the abundance evolution. Both the volume (light line) and abundance (heavy line) for each model are shown relative to the volume and abundance of the fiducial model ($w = -1$ and $\Omega_M = 0.3$). Note the clear differences between changes in w and changes in Ω_M , indicating that in principle w and Ω_M can be determined simultaneously.

can do just this²¹, because the equation of state of the dark energy determines how its energy density evolves $\rho_Q \propto R^{-3(1+w)}$, where R is the scale factor. This evolution affects the expansion history of the universe, which is coupled to the volume-redshift relation and the growth rate of density perturbations³².

Fig 3 contains a plot of the Ω_M and w dependence of the yields of the SZE survey in the case that the mass limit is taken to be a constant $M_{lim} = 2 \times 10^{14} h_{50}^{-1} M_\odot$. Note (lower left) that increasing w from -1 (the Λ case) to -0.2 (with fixed $\Omega_M = 0.3$) decreases the number of clusters expected at intermediate redshifts, but increases the number expected at high redshift. This is explained in the upper left panel; at low redshift, the larger surveyed volume of the $w = -1$ model is the dominant factor, whereas at higher redshift

the evolution of the abundance plays a larger— and eventually dominant— role. The right panel contains expected yields as a function of Ω_M (with fixed $w = -1$). Lower Ω_M yields are larger, and they grow ever larger fractionally with redshift. This is essentially the result of the evolution of abundances, because the volumes probed are very similar in these models (upper right). The slower growth of density perturbations in low Ω_M models means that the abundance changes more slowly, and we expect to see clusters to higher redshift. For more realistic tests which include the cosmological dependence of the limiting mass $M_{lim}(z)$, please see Haiman, Mohr & Holder (2000).

3.2 Complementary, High Precision Cosmological Constraints

Finally, we turn to consider the cosmological constraints possible from the large solid angle, deep X-ray survey proposed by G. Ricker, D. Lamb and collaborators. Although this survey extends only to a redshift $z \sim 0.7$, it will detect 10^4 clusters and provide temperature measurements for $\sim 2,000$ of these. These large numbers make for strikingly precise cosmological constraints, and having the T_x and luminosity measurements for these clusters makes it possible to test for unusual evolution models while constraining cosmological parameters²¹.

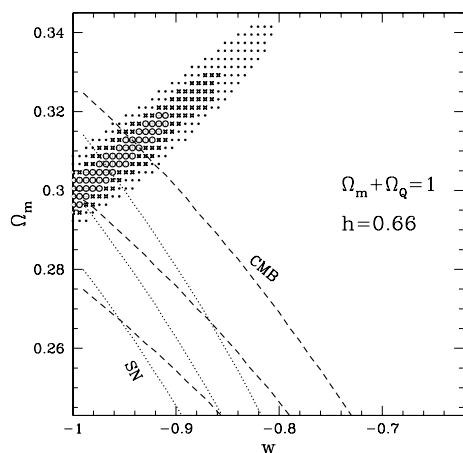


Figure 4: Here are estimates of the power contained in a large solid angle X-ray cluster survey to measure Ω_M and w simultaneously. The dots mark the 1σ , 2σ and 3σ confidence regions with which models can be differentiated from a fiducial model ($\Omega_M = 0.3$, $w = -1$, $\sigma_8 = 1$). We show only the slice of parameter space with $h = 0.66$; all models have $\Omega_M + \Omega_Q = 1$. For comparison, the dashed lines indicate the constraint from a 1% measurement of the location of the first doppler peak in the CMB anisotropy spectrum, and the dotted lines indicate the constraints from a 1% measurement of the distance to redshift $z = 1$. In combination with either the CMB or SNe Ia studies, cluster surveys enhance the constraints on w .

Fig 4 provides an estimate of the extent to which the clusters from this proposed survey will allow one to simultaneously constrain w and Ω_M . In these models we take $\Omega_M + \Omega_Q = 1$, and we require the local abundance of cluster above some mass threshold to be the same in each model. For this figure we assume some fiducial model: $\Omega_M = 0.3$, $\Omega_Q = 0.7$, $\sigma_8 = 1$, $w = -1$ and $h = 0.66$. We then use the total number of expected clusters and their redshift distribution to quantify the differences between any given model and

the fiducial model (redshifts for these clusters will be extracted from the SDSS imaging and spectroscopic survey). Note the tight, simultaneous constraints on w and Ω_M . For comparison, we show (dashed) the constraints corresponding to a 1% measurement of the location of the first Doppler peak in the CMB anisotropy spectrum, and (dotted) a 1% measurement of the distance to redshift $z = 1$. Note that the cluster survey does better than a 1% measurements to $z = 1$. In addition, the parameter degeneracies from our cluster study and these future CMB and SNe Ia constraints are roughly orthogonal, making the cluster survey complementary to either of the other studies. This orthogonality stems from the cluster survey sensitivity to abundance evolution.

3.3 Systematic Effects and Non-standard Evolution

Studies of the evolution of cluster structure are an important component of the effort to use cluster surveys to constrain cosmological parameters. The structure of cluster virial regions can affect the relation between the cluster virial mass and observables like X-ray luminosity, emission weighted ICM temperature and SZE flux. Very specific evolution models follow from theoretical work, and the observations required to test these models are now more readily available. Nevertheless, still uncertain physics, such as the effects of heating of the intergalactic medium before cluster formation, provides a potential source of systematic error in interpreting cluster surveys; we and others are currently studying these effects using hydrodynamical simulations⁴. The enormous successes in modeling galaxy clusters to date and the vast array of data soon to be available on intermediate and high redshift clusters lead me to adopt an optimistic view; I suspect that through further enhancing the hydrodynamical cluster simulations, we can tackle the finer points of cluster evolution and cosmology simultaneously.

Acknowledgments

JJM is supported by the Chandra Fellowship grant PF8-1003, awarded through the Chandra Science Center. The Chandra Science Center is operated by the Smithsonian Astrophysical Observatory for NASA under contract NAS8-39073. ZH is supported by NASA through the Hubble Fellowship grant HF-01119.01-99A, awarded by the Space Telescope Science Institute, which is operated by the Association of Universities for Research in Astronomy, Inc., for NASA under contract NAS 5-26555.

References

1. Abell, G.O. 1958, ApJ Supp, 3, 211
2. Annis, J. et al., 2000, in prep
3. Arnaud, M. & Evrard, A.E. 1999, MNRAS, 305, 631
4. Bialek, J., Evrard, A.E., Hoffman, M. & Mohr, J.J., in preparation
5. Bryan, G.L. & Norman, M.L. 1998, ApJ, 496, 80
6. Bryan, G.L. et al., in prep
7. Burles, S. & Tytler, D. 1998, ApJ, 499, 699
8. Carlberg, R.G., Yee, H.K.C. & Ellingson, E. 1997, ApJ, 478, 462
9. Cavaliere, A., Menci, N. & Tozzi, P. 1998, ApJ, 501, 493
10. David, L.P., Jones, C. & Forman, W. 1995, ApJ, 445, 578
11. Dodelson, S. & Knox, L. 2000, PRL in press (astro-ph/9909454)
12. Dressler, A. & Shectman, S. 1988, AJ, 95, 985
13. Edge, A.C., Stewart, G.C. & Fabian, A.C. 1990, MNRAS, 245, 559
14. Evrard, A.E., Mohr, J.J., Fabricant, D.G. & Geller, M.J. 1993, ApJ, 419, L9
15. Evrard, A.E., Metzler, C.A. & Navarro, J.F. 1996, ApJ, 469, 494
16. Evrard, A.E. 1997, MNRAS, 292, 289
17. Forman, W., Bechtold, J., Blair, W., Giacconi, R., van Speybroeck, L. & Jones, C. 1981, ApJ, 243, 133
18. Frenk, C.S. et al. 1999, ApJ, 525, 554
19. Geller, M.J. & Beers, T.C. 1982, PASP, 94, 421
20. Grego, L., Carlstrom, J.E., Reese, E.D., Holder, G.P., Holzzapfel, W.L., Joy, M.K., Mohr, J.J., & Patel, S. 2000, ApJ, submitted
21. Haiman, Z., Mohr, J.J. & Holder, G.P. 2000, ApJ, submitted (astro-ph/0002336)
22. Holder, G.P., Mohr, J.J., Carlstrom, J.E., Evrard, A.E. & Leitch, E.M. 2000, ApJ, submitted (astro-ph/9912364)
23. Horner, D.J., Mushotzky, R.F. & Scharf, C.A. 1999, ApJ, 520, 78
24. Jørgensen, I., Franx, M. & Kjærgaard, P. 1996, MNRAS, 280, 167
25. Lewis, A.D., Ellingson, E., Morris, S.L. & Carlberg, R.G. 1999, ApJ, 517, 587
26. Loh, E.D. & Spillar, E.J. 1986, ApJ, 307, 1
27. Mohr, J.J., Evrard, A.E., Fabricant, D.G. & Geller, M.J. 1995, ApJ, 447, 8
28. Mohr, J.J. & Evrard, A.E. 1997, ApJ, 491, 13
29. Mohr, J.J., Mathiesen, B. & Evrard, A.E. 1999, ApJ, 517, 627
30. Mathiesen, B., Evrard, A.E. & Mohr, J.J. 1999, ApJ, 520, L21
31. Newman, J.A. & Davis, M. 2000, ApJ, in press (astro-ph/9912366)
32. Peebles, P.J.E., 1980, *The Large-Scale Structure of the Universe*, (Princeton: Princeton Series in Physics)
33. Perlmutter, S. et al. 1999, ApJ, 517, 565
34. Ponman, T.J., Cannon, D.B. & Navarro, J.F. 1999, Nature, 397, 135
35. Roettiger, K., Burns, J.O. & Stone, J.M. 1999, ApJ, 518, 603
36. Roettiger, K., Stone, J.M. & Mushotzky, R.F. 1998, ApJ, 493, 62
37. Romer, A.K., Viana, P.T.P., Liddle, A.R., Mann, R.G. 2000, ApJ, in press (astro-ph/9911499)
38. Schmidt, B.P. et al. 1998, ApJ, 507, 46
39. Tolman, R.C. 1934, *Relativity Thermodynamics and Cosmology* (Oxford: Clarendon Press)
40. White, S.D.M., Navarro, J.F., Evrard, A.E. & Frenk, C.S. 1993, Nature, 366, 429
41. White, D.A. & Fabian, A.C. 1995, MNRAS, 273, 72